

# Journal of Materials Chemistry C

Accepted Manuscript



This is an *Accepted Manuscript*, which has been through the Royal Society of Chemistry peer review process and has been accepted for publication.

*Accepted Manuscripts* are published online shortly after acceptance, before technical editing, formatting and proof reading. Using this free service, authors can make their results available to the community, in citable form, before we publish the edited article. We will replace this *Accepted Manuscript* with the edited and formatted *Advance Article* as soon as it is available.

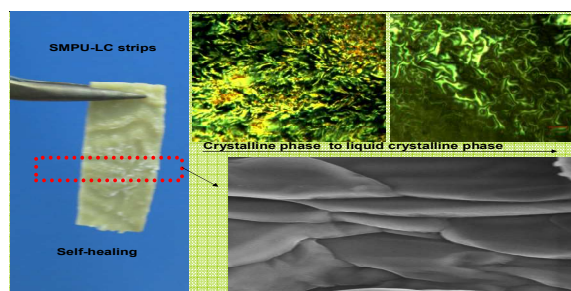
You can find more information about *Accepted Manuscripts* in the [Information for Authors](#).

Please note that technical editing may introduce minor changes to the text and/or graphics, which may alter content. The journal's standard [Terms & Conditions](#) and the [Ethical guidelines](#) still apply. In no event shall the Royal Society of Chemistry be held responsible for any errors or omissions in this *Accepted Manuscript* or any consequences arising from the use of any information it contains.

# Development of liquid-crystalline shape-memory polyurethane composites based on a semi-crystalline reversible phase and hexadecyloxybenzoic acid for self-healing applications

Shaojun Chen<sup>1</sup>, Hongming Yuan<sup>1</sup>, Haitao Zhuo<sup>2</sup>, Shiguo Chen<sup>1</sup>, Haipeng Yang<sup>1</sup>, Zaochuan Ge<sup>\*1</sup>, and Jianhong Liu<sup>\*2</sup>

## Table of contents



Novel liquid crystalline shape memory polyurethane composites display liquid crystalline properties, triple-shape memory behaviours and self-healing behaviours

**Development of liquid-crystalline shape-memory polyurethane composites based on polyurethane with semi-crystalline reversible phase and hexadecyloxybenzoic acid for self-healing applications**

Shaojun Chen<sup>1</sup>, Hongming Yuan<sup>1</sup>, Haitao Zhuo<sup>2</sup>, Shiguo Chen<sup>1</sup>, Haipeng Yang<sup>1</sup>, Zaochuan Ge<sup>\*1</sup>, and Jianhong Liu<sup>\*2</sup>

<sup>1</sup>Shenzhen Key Laboratory of Special Functional Materials, Shenzhen Engineering Laboratory for Advanced Technology of Ceramics, College of Materials Science and Engineering, Shenzhen University, Shenzhen, 518060, China. <sup>2</sup>Shenzhen Key Laboratory of Functional Polymer, College of Chemistry and Chemical Engineering, Shenzhen University, Shenzhen, 518060, China.

\*Corresponding author: College of Materials Science and Engineering, Shenzhen University, Shenzhen 518060, China. Tel or Fax: +86-755-26534562. E-mail: gezc@szu.edu.cn; liujh@szu.edu.cn ;

Electronic Supplementary Information (ESI) available:

Video A\*. Self-assemble and move spontaneously of LC-SMPU composite at liquid crystalline state

Fig. A\*. DSC curves of pure HOBA (a), and pure PHA-based SMPU(b)

Fig B\*. WAXD of sample SMPU-0.8HOBA at different temperature upon heating

Fig. C\*.  $\tan\delta$  curves of LC-SMPU composites with different HOBA content

Fig. D\*. Strain-time-temperature curves of LC-SMPU composites for triple-shape memory effects

Fig. E\*. Visualization image (100 $\times$ ) of LC-SMPU composites showing the sealed fracture

**Abstract:**

Shape memory materials and self-healing materials have attracted considerable attentions in recent years. This paper reports the development of a liquid-crystalline shape-memory-polyurethane (LC-SMPU) composite based on SMPU and hexadecyloxybenzoic acid (HOBA) for self-healing applications. The results demonstrate that the HOBA is physically mixed with SMPU having a semi-crystalline reversible phase to form LC-SMPU composites. The two-phase separated structure comprises an SMPU matrix and a HOBA phase. The HOBA phase exhibits a reversible nematic phase within a temperature range of 101-130°C, while the SMPU matrix acts as a stable polymeric film for various applications. Both the semi-crystalline soft phase of the SMPU matrix and the HOBA crystalline phase can be used to trigger shape memory effects. The LC-SMPU composites display not only triple-shape memory behaviours but also self-healing behaviours due to the heating-induced “bleeding” behaviour of HOBA in the liquid crystalline state and their subsequent recrystallisation upon cooling.

**Keywords:** liquid crystalline, shape memory, polyurethane, composite, self-healing,

**Introduction**

Stimuli-responsive polymers play an important role in many applications, such as diagnostics, drug delivery, ‘smart’ optical systems and tissue engineering, as well as in micro-electromechanical systems, biosensors, textiles and coatings<sup>1</sup>. As one of the most important stimuli-responsive polymers, shape-memory polymers (SMPs) can adopt temporary shapes and recover their original shapes upon exposure to external stimuli.<sup>2,3</sup> To date, numerous SMPs based on various structures have been developed, including polyurethane, polystyrene copolymer and epoxy-based polymers. The filling of shape memory polymer composites (SMPCs) with different fillers also broadens the varieties and functionalities of SMPs, significantly expanding their applications<sup>3</sup>. In addition to their basic reinforcement functionalities and athermal stimuli-responsive effects, several SMPCs were

recently reported to enable advanced shape-memory effects (SMEs), including spatially controlled SMEs, multiple SMEs and two-way SMEs.<sup>4</sup> These new functionalities make SMPCs increasingly useful in both scientific studies and industry applications.

SMPC fillers primarily include organic agents, such as azobenzene derivatives, inorganic/metallic particles, such as carbon nanotubes, and polymers, such as poly(ethylene glycol)<sup>3</sup>. As important functional filler, liquid crystals are widely used to fabricate various liquid crystalline polymer composites that combine the basic properties of conventional polymers with those of liquid crystals<sup>5, 6</sup>. However, to date, few studies have examined SMPCs with liquid crystal fillers. The studies on SMPs with liquid crystalline properties have primarily focused on liquid-crystalline elastomers or polymers for two-way SMEs or triple SMEs<sup>7-9</sup>. The study of thermotropic liquid-crystalline polyurethane has been limited to reinforcement in shape-memory polyurethanes (SMPUs).<sup>10</sup> However, recently, Chen et al. developed a controllable strategy to synthesise a triple-shape memory supermolecular composite via H-bonding interactions between a polymer and mesogenic units.<sup>11</sup> More recently, we developed another liquid-crystalline SMPC based on an amorphous reversible phase and hexadecyloxybenzoic acid (HOBA)<sup>12</sup>. Preliminary results suggested that the reported liquid-crystalline SMPCs had both triple-shape memory properties and liquid-crystalline properties. These studies inspired us to continue to develop liquid-crystalline SMPCs with advanced functionalities for more applications.

Furthermore, recent advances in materials and polymer chemistry have led to the development of mendable or healable polymers that exhibit the ability to undergo self-repair or self-healing<sup>13-15</sup>. Martien et al. proposed that the emerging applications of stimuli-responsive polymers include smart and self-healing coatings<sup>1</sup>. Ghosh et al. also suggested that self-healing materials with the ability to repair themselves in less than an hour can be used in many applications, ranging from decoration to the biomedical industries<sup>16</sup>. In previous reports, Li et al. developed SMP-based syntactic foam and foam cored sandwich structures for the purpose of self-healing impact damage repeatedly. They also performed a solid thermo-mechanical characterisation for using SMP-based composites to self-repair macro-length scale damage<sup>17, 18</sup>. In addition, Kohlmeyer et al. developed reversibly tunable SMP functions, including material re-sealability, in a single SMP

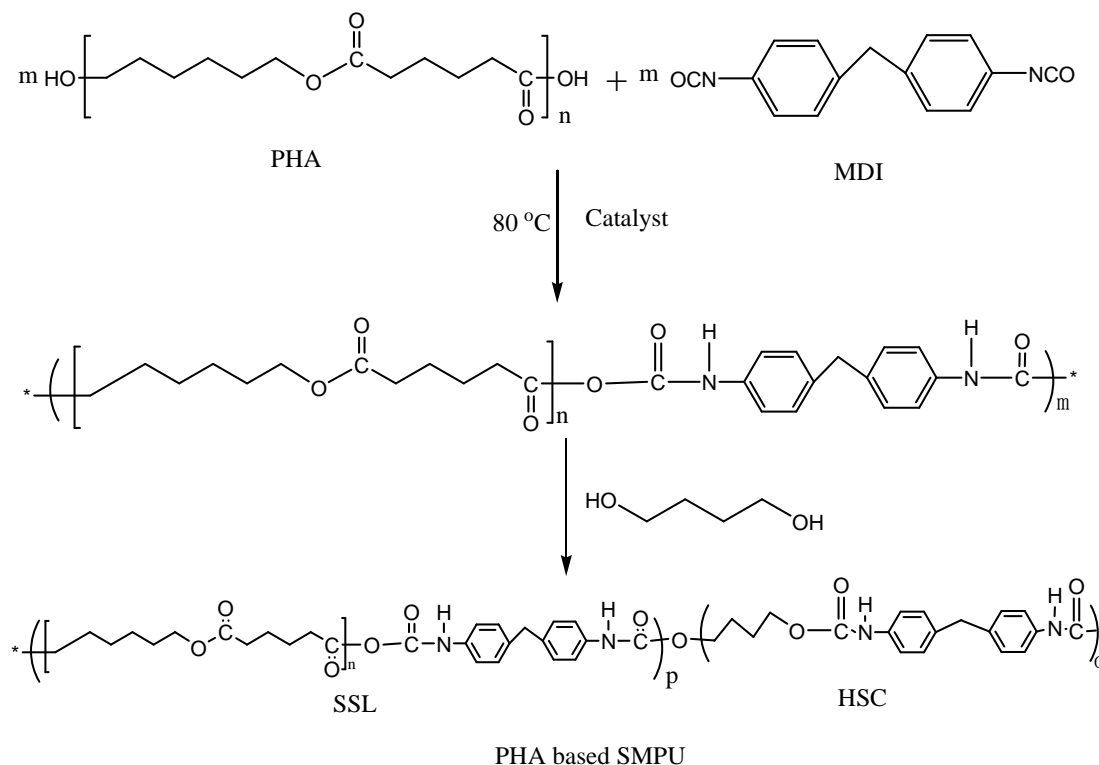
nanocomposite.<sup>19</sup> However, the most straightforward approach to repairing damage in polymeric objects involves liquefying the materials by heating to a temperature above their glass transition or melting temperature or by exposing them to a plasticising solvent. The liquid state of the polymer then allows for surface rearrangement in the damaged area, followed by wetting between surfaces, and, finally, diffusion and re-entanglement of the polymer chains<sup>20</sup>. For example, Luo et al. reported an epoxy/polycaprolactone (PCL) phase-separated blend exhibiting thermal mending and reversible adhesion<sup>21</sup>. In this system, heating-induced “blending” behaviour was observed in the form of spontaneous wetting of all free surfaces by the molten PCL phase, and this bleeding was capable of repairing damage by crack-wicking and subsequent recrystallisation with only minor concomitant softening. In addition, Sanchez et al. reported that spontaneous motion was observed in hierarchically assembled active matter, such as conventional polymer gels, liquid crystals and emulsions<sup>22</sup>. Agrawal et al. also reported dynamic self-stiffening in liquid crystal elastomers for the development of self-healing materials<sup>23</sup>. These studies suggest that the shape memory behaviours of polymers, the recrystallisation behaviour of crystals and the spontaneous motion or self-stiffening of liquid crystals can be used to design self-healing materials.

In our earlier report, liquid-crystalline SMPCs filled with HOBA were reported to possess both an SMPU amorphous phase and a HOBA crystallisable phase. The HOBA phase exhibited a reversible nematic liquid crystalline phase, crystal melting transitions upon heating and recrystallisation upon cooling<sup>12</sup>. According to the mechanisms of self-healing materials described above, the HOBA phase can be used to self-heal nano-scale cracks or even macro-length scale damages because it undergoes spontaneous motion in the liquid crystalline state upon heating and recrystallisation upon cooling. Therefore, in this study, another liquid-crystalline SMPC was developed for seal-healing applications. Different from the previous system, SMPU with a semi-crystalline reversible phase, i.e., a  $T_m$ -type SMPU, was first prepared and then selected as the polymer matrix in this experiment. HOBA was chosen as the liquid crystal mesogen because it exhibits good crystallisability and an exclusively reversible nematic liquid-crystalline phase.<sup>21-23</sup> Thus, a series of liquid-crystal shape-memory polyurethane composites, termed LC-SMPU composites, were prepared by adding different concentrations of HOBA to the  $T_m$ -type SMPUs. This study investigated the

structure, morphology and properties, including the shape-memory and self-healing behaviours, of LC-SMPU composites based on SMPU with a semi-crystalline reversible phase and HOBA.

## 2. Experimental Part

### 2.1 Synthesis of $T_m$ -type SMPU



**Scheme 1.** Synthesis route for PHA-based SMPU

Poly(1,6-hexamethylene adipate) (PHA,  $M_n=4000$ ), methylene diphenyl diisocyanate (MDI), dimethylformamide (DMF, HPLC) and 1,4-butanediol (BDO) were bought from Aladdin Reagents Co., Ltd. (Shanghai). The  $T_m$ -type SMPU with 25 wt% hard segment (MDI-BDO segment) content was synthesised by a bulk polymerisation method with MDI, BDO and PHA according to procedures described in the literature.<sup>24, 25</sup> The synthesis method is presented in **Scheme 1**. Typically, 75.0 g of PHA was mixed with 19.6 g of MDI at  $80\text{ }^\circ\text{C}$  for 30 min, followed by chain extension with 5.38 g of BDO for another 30 min. Thereafter, the resulting prepolymer was poured onto a Teflon pan for a post-curing process at  $100\text{ }^\circ\text{C}$  in a vacuum oven. Finally, the bulk SMPU resin was obtained after post-curing for 10 hours.

### 2.2 Preparation of LC-SMPU composites

A 10 wt% SMPU/DMF solution was first prepared by dissolving the obtained bulk PHA-based SMPU resin ( $M_n=89,000\text{g/mol}$ ) in DMF for 24 h at  $80^\circ\text{C}$ . According to the composition of the LC-SMPU composites illustrated in Table 1, a certain quantity of HOBA, e.g., 1.68 g, was added to the SMPU/DMF solution containing approximately 10.0 g of SMPU resin. Under strong mechanical stirring, the SMPU and HOBA were mixed for 2 hours to obtain a homogenous solution-phase mixture. Finally, samples of the LC-SMPU composite for the following tests were obtained by casting the mixture onto a Teflon pan, which was then baked at  $80^\circ\text{C}$  for 24 hours and further dried at  $80^\circ\text{C}$  under a vacuum of 0.1-0.2 kPa for 24 hours. The samples were coded as SMPU-#HOBA, in which # is the molar ratio of HOBA/MDI, e.g., sample SMPU-0.4HOBA.

Table 1. Composition of LC-SMPU composites based on  $T_m$ -type-SMPU and HOBA

Samples	SMPU* (g)	HOBA (g)	HOBA content (wt%)	Molar ratio of HOBA/MDI
Pure SMPU	10	--	--	--
SMPU-0.2HOBA	10	1.68	14.4	0.2
SMPU-0.4HOBA	10	3.36	25.1	0.4
SMPU-0.6HOBA	10	5.04	33.5	0.6
SMPU-0.8HOBA	10	6.72	40.2	0.8
SMPU-1.0HOBA	10	8.40	45.7	1.0

\* SMPU is PHA based SMPU with 25wt% hard segment content.

### 2.3 Structural characterisation

FT-IR spectra were collected using a Nicolet 760 FT-IR spectrometer by the FT-IR attenuated total reflection (ATR) method. Ten scans at  $4\text{ cm}^{-1}$  resolution were signal averaged and stored as data files for further analysis. Smooth films with a thickness of 0.2 mm were used.

Wide angle X-ray diffraction (WAXD) measurements were performed on a D8 Advance (Bruker, Germany) with an X-ray wavelength of 0.154 nm at a scanning rate of  $12^\circ/\text{min}$ . Specimens with 0.5 mm thickness were prepared for these measurements.



DSC curves were determined using a TA Q200 instrument with nitrogen purge gas. Indium and zinc standards were used for calibration. Samples were first heated from  $-60^{\circ}\text{C}$  to  $200^{\circ}\text{C}$  at a heating rate of  $10^{\circ}\text{C}/\text{min}$ , kept at  $200^{\circ}\text{C}$  for 1 min, and then cooled to  $-60^{\circ}\text{C}$  at a cooling rate of  $10^{\circ}\text{C}/\text{min}$ , and finally, a second heating scan from  $-60^{\circ}\text{C}$  to  $200^{\circ}\text{C}$  was performed.

The identification of mesophases and the determination of the phase transition temperatures were performed using a Zeiss-Axioskop polarised optical microscope (POM) equipped with a Linkam-THMS-600 variable-temperature stage at a scan rate of  $2^{\circ}\text{C}/\text{min}$  by heating from  $20^{\circ}\text{C}$  to  $150^{\circ}\text{C}$  and cooling from  $150^{\circ}\text{C}$  to  $20^{\circ}\text{C}$  under cool air.

The morphology of the samples was examined using Scanning Electron Microscopy (SEM, Hitachi, Japan). Prior to scanning, the samples were coated with a thin layer of gold.

The dynamic mechanical properties of the samples were determined using a PerkinElmer DMA at 1 Hz with a heating rate of  $2^{\circ}\text{C}/\text{min}$  from  $-60^{\circ}\text{C}$  to  $150^{\circ}\text{C}$ . Specimens were prepared for DMA testing by casting a film with a thickness of 0.5 mm, a width of 5 mm, and a length of 25 mm.

A stereo-optical microscope (VHX-600, Japan) with a hot stage (Mettler Toledo FP90 Central Processor and FP82 Hot Stage) were used to observe and record the shape recovery or self-healing process of the sample film. The heating rate of the measurement was 2 K/min.

### 3. Results and Discussion

#### 3.1. Structural analysis

In this LC-SMPU composite, the polymer matrix comprised PHA-based SMPU and the filler comprised HOBA mesogen. The structures of the LC-SMPU composites were first investigated with FT-IR and WAXD. Figure 1(A-B) shows the FT-IR spectra of the LC-SMPU composites compared with those of the pure SMPU and pure HOBA. The O-H stretching vibration was detected at approximately  $3444\text{ cm}^{-1}$  in the pure HOBA spectrum. The N-H stretching vibration indicating the formation of urethane groups was observed at approximately  $3317\text{ cm}^{-1}$  in the pure SMPU spectrum. In the LC-SMPU composites, e.g., sample SMPU-0.8HOBA, not only were the O-H and N-H stretching vibrations detected at the same frequencies, but the C=O stretching vibrations exhibited two strong absorption peaks: one at  $1720\text{ cm}^{-1}$ , which belongs to the urethane groups of SMPU, and the other at

1675  $\text{cm}^{-1}$ , corresponding to the aromatic carboxylic acid groups of HOBA<sup>24</sup>. Additionally, the sample SMPU-0.8HOBA displayed new frequencies at approximately 1012  $\text{cm}^{-1}$  and 946  $\text{cm}^{-1}$ . These frequencies were also observed in the spectrum of pure HOBA. Of them, the frequency at approximately 1012  $\text{cm}^{-1}$  arises from the C-O stretching vibration of acids. Thus, the FT-IR spectra confirmed that the HOBA had successfully incorporated into the PHA-based SMPU to form LC-SMPU composites. In addition, Figure 1(B) demonstrates that the new absorption peak at 1675  $\text{cm}^{-1}$  could only be detected when the molar ratio of HOBA/MDI was greater than 0.6, and no significant frequency changes in the N-H or C=O vibration frequencies were observed among the LC-SMPU composites with varying HOBA concentrations. These results imply that the incorporation of HOBA does not influence the original hydrogen bonding between the N-H group and the C=O of the urethane groups in SMPU. This observation is consistent with previous reports in that the interactions between the COOH group of 4-dodecyloxybenzoic acid and the urethane C=O and N-H groups of polyurethane are not prevalent in the polyurethane complex with 4-dodecyloxybenzoic acid<sup>21-23</sup>. Additionally, XRD patterns provided further important insights into the structural analysis. Figure 1(C) shows that the crystalline peaks of the PHA-based SMPU at 21.3° and 24.0° and the crystalline peaks of HOBA at approximately 15.6°, 17.8°, 19.8°, 22.7°, 24.5°, and 26.8° were detected in the LC-SMPU composites. Compared with the pure HOBA, the majority of the crystalline peaks shifted to higher  $2\theta$  values, particularly in the samples SMPU-0.2HOBA, SMPU-0.4HOBA and SMPU-0.8HOBA. This implies that the crystal face distance ( $d$ ) of HOBA becomes smaller in the LC-SMPU composites due to the interruption of the polyurethane chains. That is, HOBA crystals are distributed physically within the SMPU polymer matrix. Therefore, in this study, the LC-SMPU composite filled with HOBA is a simple physical mixture of HOBA with PHA-based SMPU. Although the formation of hydrogen bonds with the polymer matrix may improve the miscibility of the SMPU/HOBA composite, the HOBA cannot form an LC mesogen when it attaches to the polyurethane backbone. In a previous report, Chen et al. demonstrated that the liquid-crystalline mesophase was lost when LC mesogens containing pyridine moieties were attached to SMPU containing carboxyl groups through hydrogen bonding between pyridine and COOH.<sup>13</sup> Compared with previous systems, the present LC-SMPU composites tended to retain the intrinsic

liquid-crystalline properties of the HOBA mesogens because they preserved the original dimers of HOBA formed by hydrogen bonding between COOH and COOH, as shown in Figure 1(D) <sup>25</sup>.

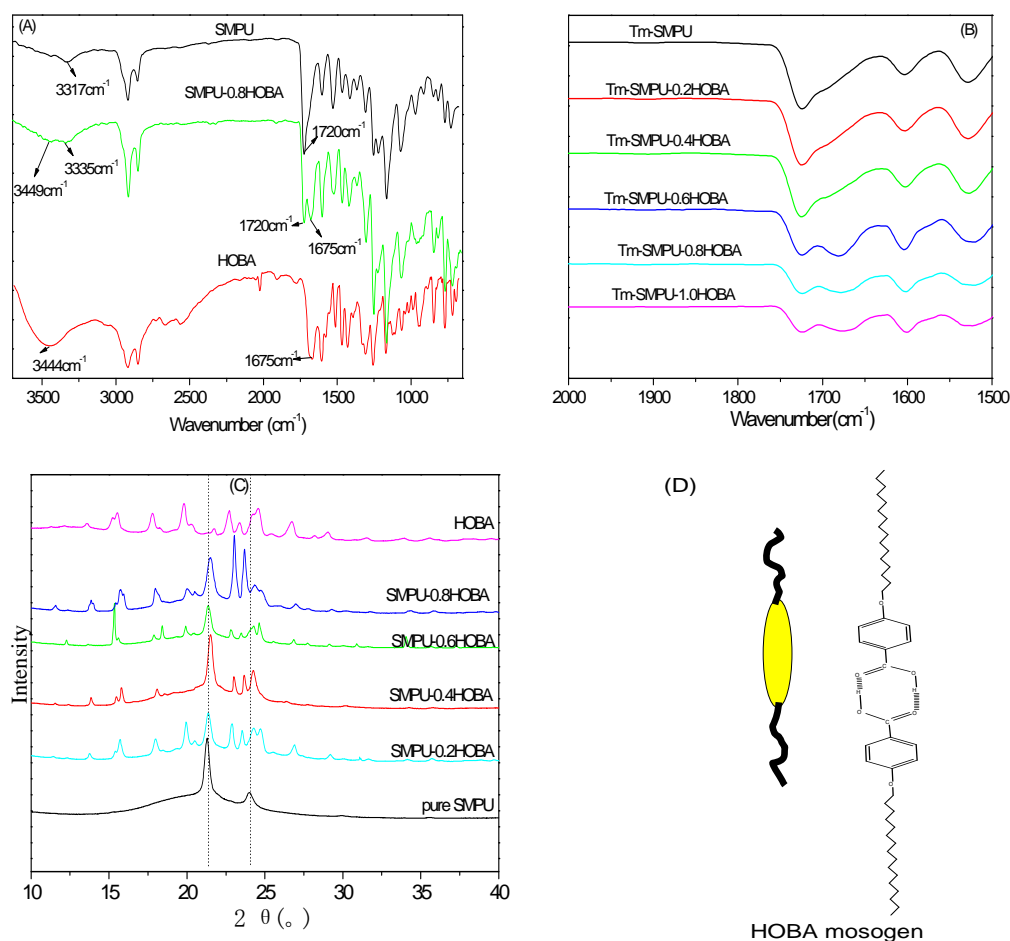


Figure 1. FT-IR spectra of the LC-SMPU composites compared with those of pure SMPU and HOBA (A), FT-IR spectra of LC-SMPU composites with varying HOBA content (B), XRD spectra of LC-SMPU composites with varying content (C) and molecular modelling of HOBA dimers via hydrogen bonding (D)

### 3.2 Thermal properties

DSC instruments have been widely used to study the thermal properties of materials, including the phase transitions of polymers. **Figure 2(A)** presents the second DSC heating curves of the LC-SMPU composites compared with those of pure PHA-based SMPU and HOBA. The pure SMPU is observed to have only a crystal melting temperature ( $T_m$ ) at approximately 42.5°C. The pure HOBA displays an exothermic peak (peak 1) at approximately 67°C; two obvious endothermic peaks (peak 2 and peak 3) at approximately

19.3°C and 101.6°C, respectively; and a weak endothermic peak (peak 4) at 130°C under this scanning condition. Peak 1 is a cold crystallisation of HOBA. Peak 2 and peak 3 show crystal melting transitions. The HOBA forms two types of crystals due to its long chains. These observations were verified in an earlier communication<sup>12</sup>. When HOBA was physically mixed with the PHA-based SMPU to form LC-SMPU composites, the  $T_m$  of the soft phase of SMPU shifted to a higher temperature, e.g., to approximately 46.5°C in the sample SMPU-0.8HOBA, as shown in Figure 2(A). The cold crystallisation (peak 1) observed in pure HOBA disappeared when the HOBA content was lowered, e.g., in samples SMPU-0.2HOBA and SMPU-0.6HOBA, as shown in Figure 2(B). In addition, the melting temperature of the first HOBA crystal shifted to ca. 92.5°C, and the melting temperature of the second HOBA crystal remained constant at approximately 101.2°C in all the LC-SMPU composites. Figure 2(B) also demonstrates that the first crystal melting peak became larger as the HOBA content increased for molar ratios of HOBA/MDI below 0.6, whereas only the second crystals were detected in the samples with higher HOBA content, e.g., samples SMPU-0.8HOBA and SMPU-1.0HOBA. The DSC cooling curves also demonstrate that the LC-SMPU composites not only formed soft-phase crystals at ca. 14.3-20.7°C but also possessed two recrystallisation peaks at approximately 70.6°C and 85.4°C when the HOBA content was lower, e.g., in sample SMPU-0.2HOBA, whereas only one recrystallisation peak was observed in samples SMPU-0.8HOBA and SMPU-1.0HOBA, as shown in Figure 2(C). These recrystallisation peaks exactly correspond to the crystal melting peaks on the second heating curves, as discussed above. That is, the HOBA crystals formed at 70.6°C will melt at 92.5°C, while the second crystal formed at 85.4°C will melt at 101.2°C. Moreover, compared with the pure SMPU (see ESI Fig. A\*), Figure 2(C) demonstrates that the recrystallisation temperature of the soft phase shifted to a higher temperature on the cooling curves as the HOBA content increased. Compared with the pure HOBA, both the recrystallisation temperature and melting temperature of the first HOBA crystals shifted to higher temperatures because the crystal seeds were able to form easily inside the polyurethane matrix and the HOBA crystals exhibited greater stability. This hypothesis was also substantiated by the DSC of LC-SMPU composites based on an amorphous soft phase, as reported in literature<sup>12</sup>. Because the recrystallisation of the soft segment of the  $T_m$ -type

SMPU was accompanied by the formation of HOBA crystals at 70.6°C, the formed crystals then melted at 92.5°C upon heating. We thus confirmed that the first type of HOBA crystal was easily formed in the LC-SMPU composites because the HOBA was captured by the polyurethane matrix. The polyurethane chains promoted the formation of crystal seeds of HOBA. In contrast, the formed HOBA crystals also promote the assembly of the soft segment of SMPU, enhancing the crystal stability of the soft phase. However, the second HOBA crystals were formed at ca. 85.4-86.8°C on the cooling curves (see Figure 2(C)), and the second crystal melting temperature appeared at approximately 101°C on the second DSC heating curve (see Figure 2(B)). These two temperatures are very close to the recrystallisation temperature and the melting temperature of the second crystals in the pure HOBA, indicating that the first crystals were formed by the captured HOBA molecules and that the second crystals primarily comprised free HOBA crystals in the LC-SMPU composites.

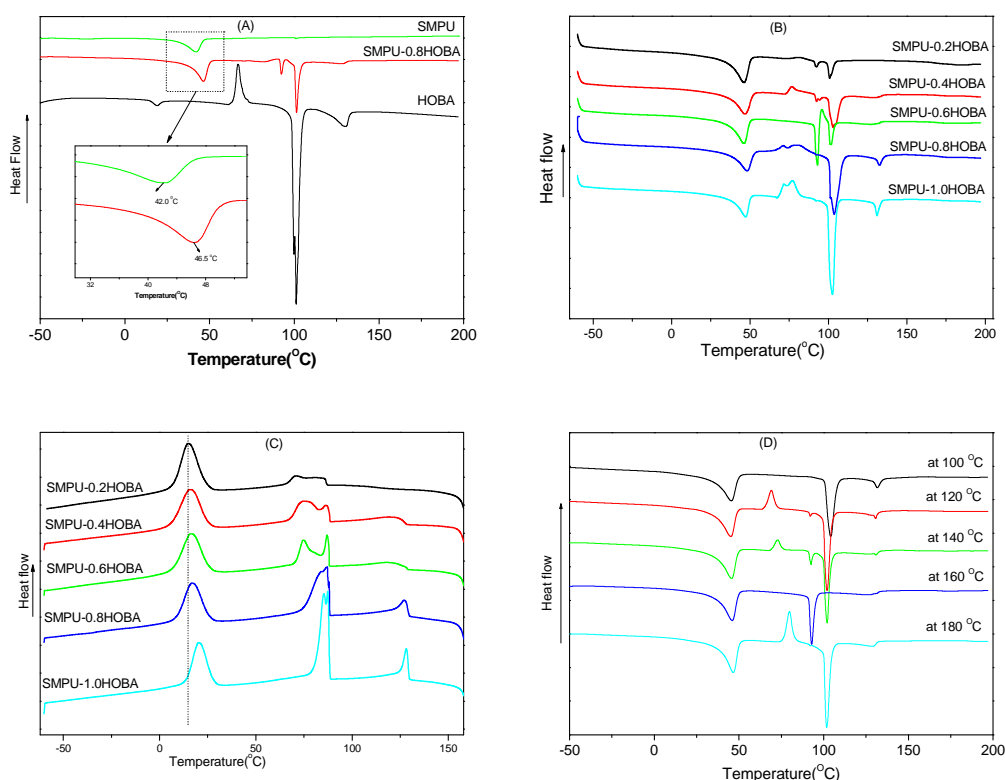


Figure 2. the second heating DSC curves of SMPU-0.8HOBA compared with the pure SMPU and HOBA (A); the second heating DSC curves of LC-SMPU composites with different HOBA content (B); the cooling DSC curves of LC-SMPU composites with different HOBA content (C) ; and the second heating DSC curves of SMPU-0.4HOBA at different annealing temperature(D).



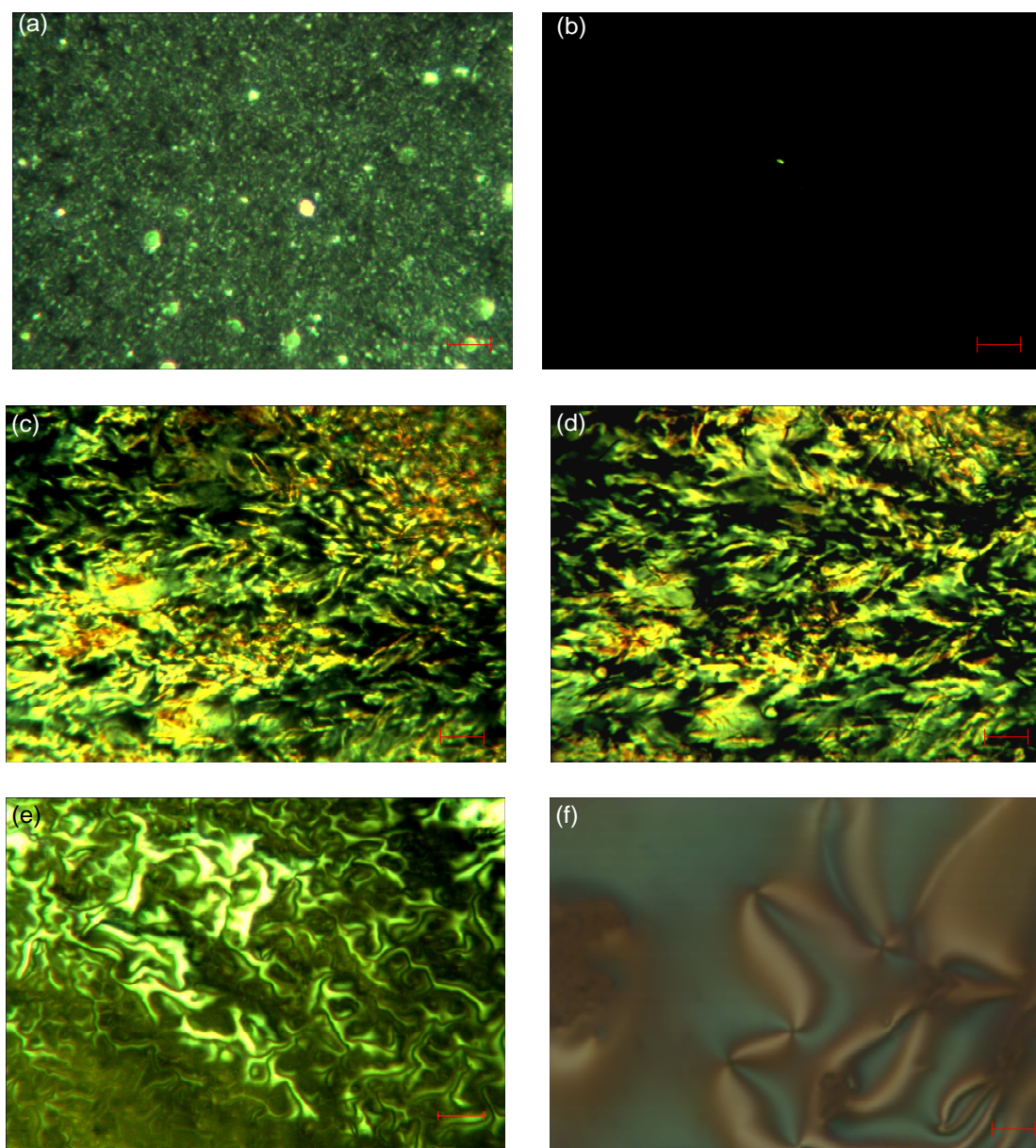


Figure 3. POM images (400 $\times$ ) of pure SMPU at different temperatures [30 $^{\circ}$ C for semi-crystalline phase (a); 50 $^{\circ}$ C for isotropic phase without crystals(b)], sample SMPU-0.8HOBA at different temperatures [30 $^{\circ}$ C for crystalline phase(c); 50 $^{\circ}$ C crystalline phase (d)]; 120 $^{\circ}$ C for nematic liquid crystalline phase (e)], and pure HOBA at 120 $^{\circ}$ C for nematic liquid crystalline phase (f)

The effects of heat treatment were further investigated by DSC. The sample SMPU-0.6HOBA was first heated to 100 $^{\circ}$ C, followed by heating to 120 $^{\circ}$ C, 140 $^{\circ}$ C, 160 $^{\circ}$ C and 180 $^{\circ}$ C. After cooling to -60 $^{\circ}$ C, the second heating curve from -60 $^{\circ}$ C to 200 $^{\circ}$ C was recorded for analysis. Figure 2(D) shows the second DSC heating curves of the sample SMPU-0.4HOBA treated with different annealing temperatures. Similar to the results of the LC-SMPU composites with an amorphous reversible phase<sup>12</sup>, Figure 2(D) demonstrates that

the enthalpy of the first type of HOBA crystals was small when the annealing temperature was lower than 140°C and that it increased significantly when the annealing temperature was higher than 160°C in the LC-SMPU composites based on SMPU with a semi-crystalline reversible phase. This effect may be due to the ability of higher annealing temperatures to promote HOBA molecules to enter the polyurethane chain due to their lower viscosity at higher temperatures. However, annealing temperatures above 180°C caused the HOBA molecules to escape from the polyurethane chain. Only free HOBA crystals could be detected in the second heating curves following thermal treatment at higher temperatures, as shown in Figure 2(D). We thus confirmed that the doped HOBA was divided into two parts: one portion of the HOBA molecules was captured or wrapped by the polyurethane chain due to the strong Van der Waals interaction between HOBA and the PHA soft segment, and the other portion was present as free HOBA. The captured HOBA was strongly influenced by the polyurethane chain, whereas the free HOBA retained its intrinsic crystalline and liquid-crystalline properties.

### 3.3 Liquid-crystalline properties

The phase transition behaviours of the LC-SMPU composites were further investigated with POM. Before testing, all specimens were cooled to room temperature for 24 hours after being heated to their isotropic phase. The POM images at different temperatures during the heating process were recorded for analysis. Figure 3(a-b) presents the POM images of pure, PHA-based SMPU at different temperatures upon heating. POM images of PHA-based SMPUs with various soft segment lengths and hard segment contents have been investigated systematically in previous literature<sup>26</sup>. In this study, the POM images demonstrated that the pure SMPU with 25 wt% hard segment content exhibited a semi-crystalline texture with right-angled intersection extinction phenomenon below 30°C; an isotropic texture appeared when the temperature was higher than 50°C. This observation is consistent with the DSC results above as the semi-crystalline soft phase of SMPU melted above 42.5°C. However, the sample SMPU-0.8HOBA maintained its bright and colourful crystalline texture until the temperature reached 100°C. This semi-crystalline texture changed slightly when the sample was heated from 30°C to 50°C, as shown in Figure 3 (c-d). The temperature-dependent WAXD pattern also confirmed that HOBA was in a crystalline state

below 60°C (see **ESI Fig. B\***). When the temperature was increased to a range from 100°C to 130°C, the POM image presented a typical schlieren texture of the nematic phase, as shown in Figure 3(e). This nematic schlieren texture was repeated when the temperature cooled to below 130°C. These schlieren textures are also very similar to those of pure HOBA, as shown in Figure 3(f), indicating that the liquid-crystalline phase of the LC-SMPU composites can be attributed to the doped HOBA phase. Compared with pure HOBA, the LC-SMPU composites not only retain the intrinsic liquid-crystalline properties of HOBA but can also form a stable film for various applications as polymeric film materials. Moreover, the POM images demonstrated that the HOBA bleeds from the polymeric film because HOBA mesogens can move and self-assemble spontaneously in the liquid crystalline state (see **ESI Video A\***). However, its morphology becomes fixed immediately after crystallisation upon cooling. Similar to the epoxy/PCL phase-separated blend thermal-mending system<sup>21</sup>, this spontaneous motion and recrystallisation of HOBA mesogens provides a pathway to self-repair cracks on the polymeric film.

### 3.4 Morphology

In this experiment, LC-SMPU composite films were prepared by casting mixture solutions on a smooth pan followed by drying at 80°C in an oven. Although all polymeric films are macroscopically flat, they can exhibit different surface morphologies on the microscale. Figure 4 shows SEM images depicting the surface morphologies of LC-SMPU composites with varying HOBA content. These SEM images demonstrate that the pure SMPU has a smooth surface without any holes, as shown in Figure 4(a), whereas the surface of the sample becomes rough when HOBA is doped into the LC-SMPU composite. As the HOBA content increases, the surface becomes rougher. Finally, obvious phase-separated structures are formed in the LC-SMPU composites with higher HOBA content, as shown in Figure 4(b-e). One phase is the polyurethane matrix, while the other phase is likely the HOBA crystalline phase because numerous large, roughened crystals were detected in sample SMPU-1.0HOBA, as shown in Figure 4(f). These results are consistent with the DSC and POM observations. Therefore, we confirmed that the LC-SMPU composites comprised a HOBA crystalline phase and SMPU with a semi-crystalline reversible phase at room temperature. According to the DSC and POM analyses, the HOBA crystalline phase melts and enters the nematic phase



when the temperature is raised to over 100°C; HOBA mesogens can also recrystallise into two types of crystals when the temperature is cooled to below 86.8°C. In addition, the soft phase melts above 46.6°C and crystallises below 20.7°C, while the hard phase retains the shape of the polymer film upon heating as well as cooling in the polyurethane matrix. This morphology and structure provides a prerequisite condition for shape memory and self-healing functionality.

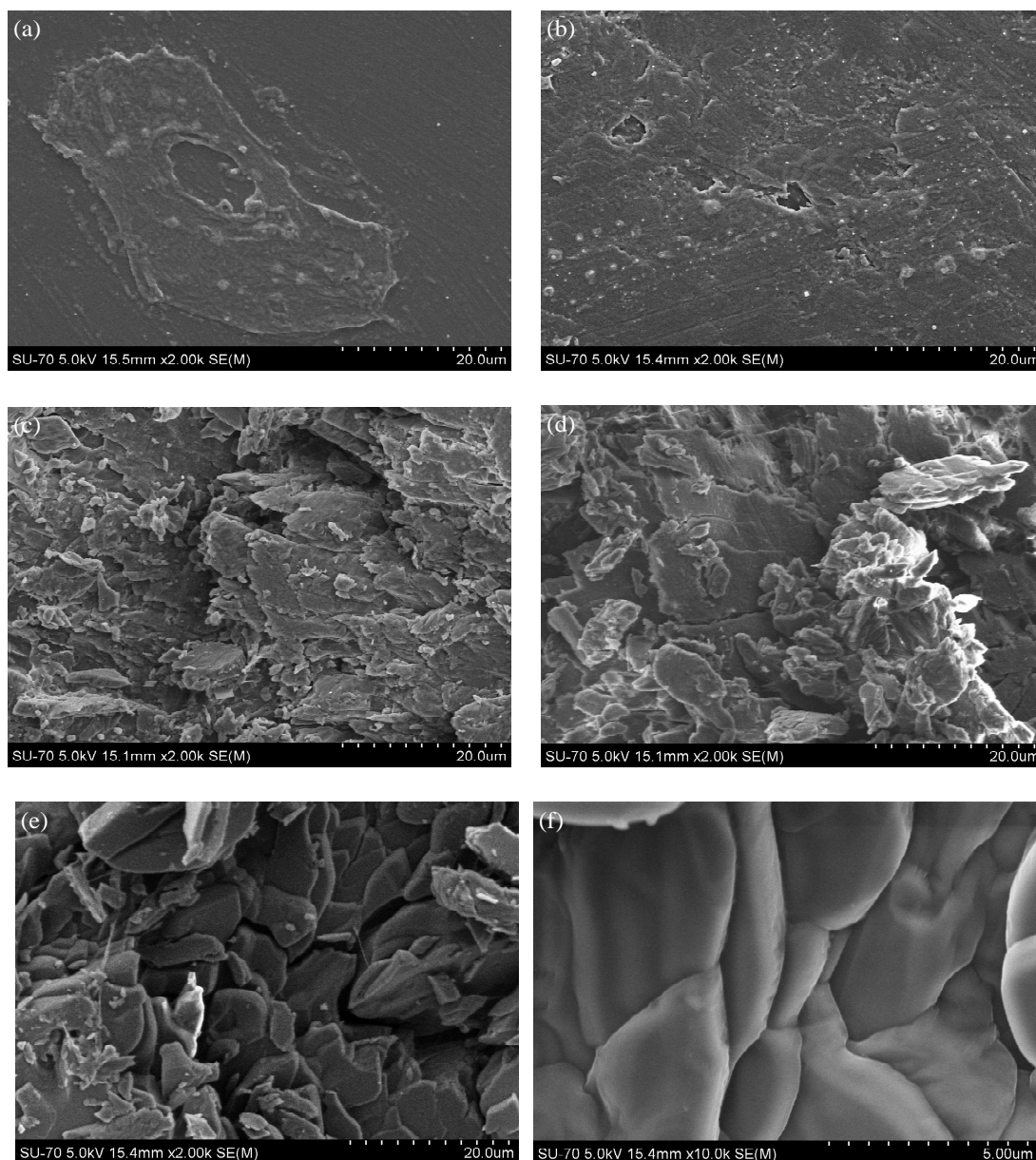


Figure 4. SEM images(5000×) of LC-SMPU composites (a-pure SMPU; b-SMPU-0.2HOBA; c-SMPU-0.4HOBA; d-SMPU-0.8HOBA; e-SMPU-1.0 HOBA; f-SMPU-1.0 HOBA (magnified picture 10,000×))

### 3.5 Dynamical-mechanical properties

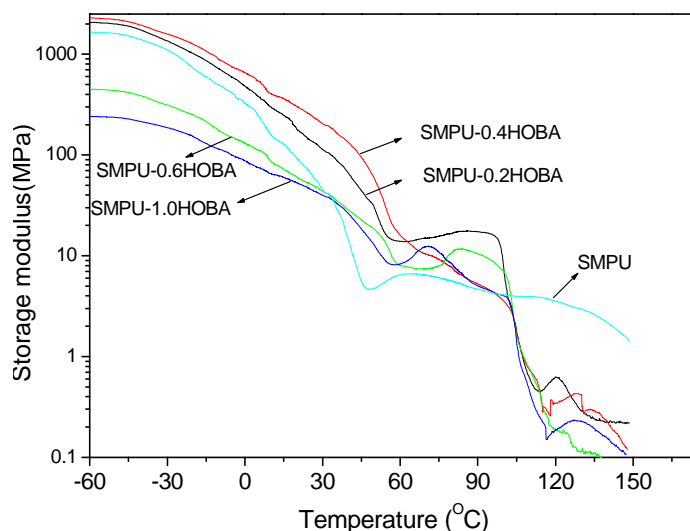


Figure 5. DMA curves of LC-SMPU composites with varying HOBA content

Another important condition for shape memory and self-healing functionality is temperature-dependent viscoelastic properties, which are primarily embodied in dynamical mechanical properties<sup>27</sup>. Figure 5 presents the DMA curves of LC-SMPU composites with varying HOBA content. The DMA curves reveal that all the samples, including the LC-SMPU composites and the pure SMPU, exhibited similar changes in the storage modulus below 90°C. The samples exhibit large glass modulus ( $E_g'$ ) values below -40°C, whereas the storage modulus values decrease gradually during the glass transition process. There is also a significant decrease in the storage modulus within the temperature range of 37°C to 48°C, as shown in Figure 5, corresponding to the crystal melting transition of the soft phase of SMPU, as observed in the DSC curves. Additionally, Figure 5 also shows that the modulus decreases in the LC-SMPU composites occurred at higher temperatures compared with the pure SMPU. This can be attributed to the better crystal stability of the LC-SMPU composites due to the crystal seeds of HOBA. However, when the temperature is raised to over 90°C, the LC-SMPU composites exhibit another significant modulus decrease within the temperature range of 90°C-118°C, while the pure SMPU maintained its stable rubbery storage modulus ( $E_r'$ ) due to the stability of its hard phase below 118°C. The LC-SMPU composites exhibited significantly increased  $\tan\delta$  values, while the pure SMPU maintained a constant value within

the same temperature range (see ESI Figure C\*). This temperature range precisely corresponds to the crystal melting transition of the HOBA crystals, further confirming that a two-phase separation structure exists in the LC-SMPU composites and that the HOBA phase can also serve as a reversible phase to trigger shape memory effects.

### 3.6 Shape memory and self-healing properties

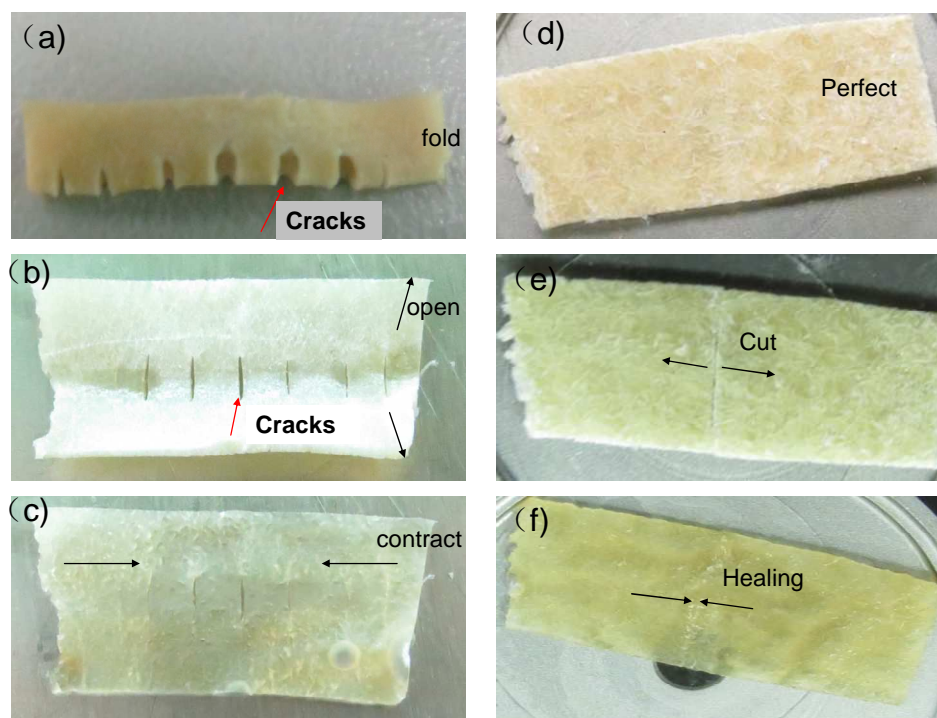
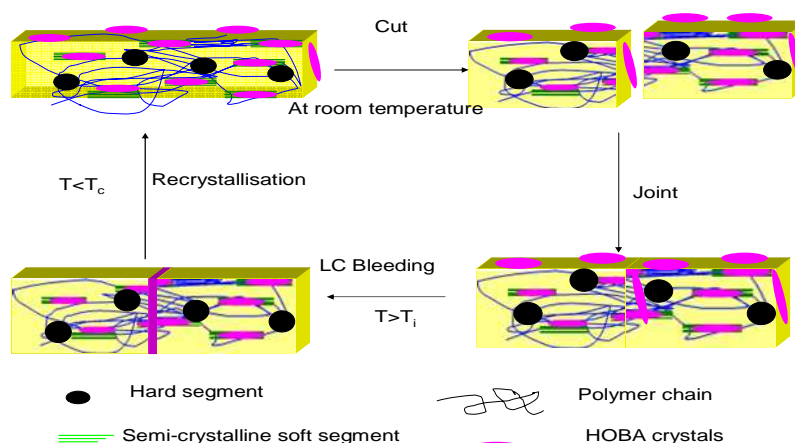


Figure 6. Triple-shape memory effect [a-the first temporary shape (folded state), with large cracks at room temperature; b-the second temporary shape (open state), after recovering from the first temporary shape at 80°C; c-the recovered shape (contracted state), after recovering from the second temporary shape at 130°C] and the thermal-induced fracture-healing process [d-original perfect strip; e-cut strip before repairing; f-self-healed strip at 120°C] of sample SMPU-0.6HOBA.

PHA-based SMPUs were reported to show good dual-shape memory effects due to the significant modulus decrease during the crystal melting transitions of the soft phase in previous studies<sup>26</sup>. As discussed above, the DMA results in our study demonstrate that the LC-SMPU composites based on SMPU with a semi-crystalline reversible phase and HOBA not only exhibit a decreasing modulus during the crystal melting transitions of the soft phase but also during the crystal melting transitions of the HOBA phase. Thus, a triple-shape memory effect is expected. However, the strain recovery in the second step was difficult to quantify due to the small recovery force above 100°C in the LC-SMPU composites (see ESI

**Fig. D\*)** arising from the low hard segment content of SMPU<sup>26</sup>. Figure 6 presents only the visualised triple-shape recovery process of the LC-SMPU composites qualitatively. Before testing, the LC-SMPU composite film (e.g., sample SMPU-0.6HOBA) was elongated to a certain length (the first temporary shape) at 110°C, then folded into a temporary strip with cracks (the second temporary shape) at 70°C. Thus, the folded strips with many cracks can be fixed after cooling to room temperature, as shown in Figure 6 (a). During the thermal-induced shape recovery process, the folded strip with cracks was observed to open itself when the temperature was raised to above 80°C, as shown in Figure 6 (b). Upon continuously increasing the temperature, the elongated strip contracted to its original shape, as shown in Figure 6(c). This behaviour constitutes a triple-shape memory effect. In addition, Figure 6(a-c) also demonstrates that the obvious cracks on the strip are healed during the shape recovery process, indicating that the LC-SMPU composite is capable of self-healing. Thus, the thermal-induced fracture-healing process of the LC-SMPU composites was further investigated in this experiment. As shown in Figure 6(d-f), a perfect strip prepared from sample SMPU-0.6HOBA was first cut into two parts before testing. The two parts were then placed together and heated to 120°C for 30 minutes. Interestingly, after cooling to room temperature, the two cut parts fused together, as shown in Figure 6(f). Even the gap between the two parts was self-healed by this thermal-treatment in the liquid crystalline state (see ESI **Fig. E\***).



Scheme 2. Thermal-induced self-healing mechanism of LC-SMPU composites based on

HOBA



According to the structure and morphology analyses above, the thermal-induced self-healing behaviour of the LC-SMPU composites can be explained by **Scheme 2**. The LC-SMPU composites contain two separated phases: the SMPU matrix and the HOBA phase. The SMPU exhibits a micro-phase separation structure composed of a semi-crystalline soft phase and a hard phase at room temperature, whereas the HOBA exhibits a crystalline phase below 100°C and a nematic liquid crystalline phase within a temperature range of 100°C to 130°C. After cutting, the two pieces of the LC-SMPU composites retained the SMPU matrix and the HOBA phase. When placed together, there was an obvious gap between the two parts prior to thermal treatment. In the nematic liquid crystalline state at high temperatures, e.g., 120°C, the HOBA mesogens bleed from the SMPU matrix and move spontaneously to the gap or cracks at the liquid crystalline state. After the HOBA mesogens recrystallise at room temperature, the gap is sealed. This self-healing process is very similar to the thermal mending of expolxy/PCL phase-separated blends<sup>21</sup>. In the present LC-SMPU composite system, the self-healing process is ascribed to the heating-induced “bleeding” behaviour of HOBA in the liquid crystalline state and its subsequent recrystallisation upon cooling.

#### 4. Conclusions

This paper proposes a type of LC-SMPU composite possessing both liquid crystalline properties and shape memory properties for novel self-healing applications. The structure, morphology and properties of the LC-SMPU composites based on SMPU with a semi-crystalline reversible phase and HOBA were investigated systematically. Structural analyses suggested that the HOBA physically mixed with the PHA-based SMPU to form LC-SMPU composites. The doped HOBA comprised two parts: captured HOBA and free HOBA. The captured HOBA was influenced significantly by the polyurethane chain, whereas the free HOBA maintained its intrinsic crystalline and liquid-crystalline properties. SEM confirmed that a two-phase separated structure comprising an SMPU matrix and a HOBA phase was formed in the LC-SMPU composites. POM demonstrated that the HOBA phase was in the nematic phase at temperatures from 101-130°C, while the SMPU matrix enabled a stable film for various applications as polymeric film materials. DMA further revealed that both the semi-crystalline soft phase of the SMPU matrix and the HOBA crystalline phase can be used to trigger shape memory effects. Therefore, the LC-SMPU composites show not only

triple-shape memory behaviour but also thermal-induced self-healing behaviour. Finally, we attributed the self-healing behaviour of this material to the heating-induced “bleeding” behaviour of HOBA in the liquid crystalline state and its subsequent recrystallisation upon cooling.

### Acknowledgements

This work was financially supported by the Natural Science Foundation of China (grant No. 21104045), the Special Research Foundation of the Shenzhen Government for Strategic Emerging Industries (grant No. JCYJ20120613102842295; GJHS20120621140852619; JCYJ20120613172439451) and the Special Research Foundation of Shenzhen Oversea High-level Talents for Innovation and Entrepreneurship (Grant No. KQCX20120807153115869). The authors would also like to thank Prof. Jean-Marie Lehn, the Nobel Prize Laureate in 1987, and Prof. Jin-lian Hu of the Hong Kong Polytechnic University for their guidance.

### References

- 1.M. A. C. Stuart, W. T. S. Huck, J. Genzer, M. Mueller, C. Ober, M. Stamm, G. B. Sukhorukov, I. Szleifer, V. V. Tsukruk, M. Urban, F. Winnik, S. Zauscher, I. Luzinov and S. Minko, *Nat. Mater.* 2010, **9**, 101-113.
- 2.J. Hu and S. Chen, *J. Mater. Chem.* 2010, **20**, 3346-3355.
- 3.H. Meng and G. Li, *Polymer* 2013, **54**, 2199-2221.
- 4.J. Hu, Y. Zhu, H. Huang and J. Lu, *Prog. Polym. Sci.* 2012, **37**, 1720-1763.
- 5.H. Huang, J. Geng, S. He, B. Li, C. Ouyang, Y. Yin, H. Cao, L. Wang, M. Hai, G. Wang and H. Yang, *Liq. Cryst.* 2007, **34**, 949-954.
- 6.M. Tatsumi, Y. Teramoto and Y. Nishio, *Biomacromolecules* 2012, **13**, 1584-1591.
- 7.P. T. Mather and K. A. Burke, *J. Mater. Chem.* 2010, **20**, 3449-3457.
- 8.L. Y. Liang, D. W. Zhou and M. G. Lu, *Adv. Liq. Cryst.* 2010, **428-429**, 391-393.
- 9.A. Lendlein, J. Zotzmann, M. Behl and D. Hofmann, *Adv. Mater.* 2010, **22**, 3424-3429.
- 10.H. M. Jeong, B. K. Kim and Y. J. Choi, *Polymer* 2000, **41**, 1849-1855.
- 11.H. Chen, Y. Liu, T. Gong, L. Wang, K. Zhao and S. Zhou, *RSC Adv.* 2013, **3**, 7048-7056.

- 12.S. Chen, H. Yuan, Z. Ge, S. Chen, H. Zhuo and J. Liu, *J. Mater. Chem. C* 2014, **2**, 1041 - 1049.
- 13.S. D. Bergman and F. Wudl, *J. Mater. Chem.* 2008, **18**, 41-62.
- 14.J. A. Syrett, C. R. Becer and D. M. Haddleton, *Polym. Chem.* 2010, **1**, 978-987.
- 15.L. R. Hart, J. L. Harries, B. W. Greenland, H. M. Colquhoun and W. Hayes, *Polym. Chem.* 2013, **4**, 4860-4870.
- 16.B. Ghosh and M. W. Urban, *Science* 2009, **323**, 1458-1460.
- 17.G. Li and N. Uppu, *Compos. Sci. Technol.* 2010, **70**, 1419-1427.
- 18.G. Li; M. John. *Compos. Sci. Technol.* 2008, **68**, 3337-3343.
- 19.R. R. Kohlmeyer, M. Lor and J. Chen, *Nano Letters* 2012, **12**, 2757-2762.
- 20.G. L. Fiore, S. J. Rowan and C. Weder, *Chem. Soc. Rev.* 2013, **42**, 7278-7288.
- 21.X. Luo, R. Ou, D. E. Eberly, A. Singhal, W. Viratyaporn and P. T. Mather, *ACS Appl. Mater. Inter.* 2009, **1**, 612-620.
- 22.T. Sanchez, D. T. N. Chen, S. J. DeCamp, M. Heymann and Z. Dogic, *Nature*, **491**, 431-434.
- 23.A. Agrawal, A. C. Chipara, Y. Shamoo, P. K. Patra, B. J. Carey, P. M. Ajayan, W. G. Chapman and R. Verduzco, *Nat. Commun.* 2013, **4**, 1739.
- 24.S. Mallakpour and M. Kolahdoozan, *E-Polymers* 2006,**1**, 257–269.
- 25.P. Wu, G. J. Deng, S. L. Xu, Q. H. Fan, L. J. Wan, C. Wang and C. L. Bai, *Chinese Sci. Bull.* 2002, **47**, 1514-1517.
- 26.S. J. Chen, J. L. Hu, Y. Q. Liu, H. M. Liem, Y. Zhu and Y. J. Liu, *J. Polym. Sci. Poly. Phys.* 2007, **45**, 444-454.
- 27.C. Liu, H. Qin and P. T. Mather, *J. Mater. Chem.* 2007, **17**, 1543-1558.